Experimental Validation of Dedicated Methods to In-Vehicle Estimation of Atmospheric Visibility Distance

Nicolas Hautière*, Didier Aubert*, Éric Dumont† and Jean-Philippe Tarel†, *IEEE Member*

Abstract

In the framework of the French project ARCOS, we developed a system using in-vehicle CCD cameras, aiming to estimate the visibility distance in adverse weather conditions, especially fog situations. The topic of this paper is the validation of the system. First, we present Koschmieder's model of apparent luminance of objects observed against background sky on the horizon and deal with the definitions of the different visibility distances we use in our measurement framework, as well as the links which bind them. Then, we describe the two specific onboard techniques we designed to estimate the visibility distance. In a third section, we present a dedicated site and how we use it to validate the previous techniques. Finally, we give results of a quantitative validation of our onboard techniques, using actual pictures of the validation site in foggy weather.

Index Terms

intelligent transportation systems, driving assistance, meteorological visibility, fog, experimental validation

* LIVIC, LCPC/INRETS, Versailles, France.

† DESE, LCPC, Paris, France.

Experimental Validation of Dedicated Methods to In-Vehicle Estimation of Atmospheric Visibility Distance

I. Introduction

Most of the information used by drivers comes from vision. It follows that reduced visibility is a cause for road accidents. A system to inform the drivers of the appropriate speed with regard to the measured weather conditions would obviously contribute to road safety. But such a system has other applications. Onboard perception equipment (cameras, radar, laser, etc.) is designed to operate within a range of conditions which is only adjustable to a certain extent. An atmospheric visibility measurement system would therefore be expected to adapt sensor operation and the associated processing (obstacle detection, lane keeping, etc.) to the prevailing weather conditions or to warn the driver that his assistance system is momentarily inoperative.

In the French project ARCOS [15], we developed such a system using onboard CCD cameras and composed of three modules. The first module detects daytime fog and estimates the meteorological visibility. The second module, which is not discussed here, uses the "v-disparity" representation [11] to detect obstacles which occult part of the road and the traffic. The last module estimates the distance to the most distant visible picture element belonging to the road surface in any conditions. One application of these methods is to automate the lighting of fog lamps, and even to adjust their intensity according to the visibility conditions.

So far, these methods were only qualitatively evaluated. Quantitative assessment has not been endeavored yet, due to the lack of a reference visibility sensor. To fill this gap, we equipped our test track in Versailles (France) with five large specific targets. The idea is to take pictures of these targets in adverse visibility conditions and to estimate the visibility distance thanks to the attenuation of their contrast. This static measurement, which uses reference targets, can then be compared to the results of our in-vehicle methods, which require no reference.

In the following, we first deal with the definitions of the different visibility distances we estimate, as well as the links which bind them. Then, our two onboard techniques are summarized.

In the third section, we present our validation site and how we use it to evaluate the previous techniques. The experimental protocol is validated by means of simulated pictures using a photometric model of fog visual effects. Finally, we give the first results of a quantitative validation using actual pictures of the validation site in foggy weather.

II. Vision and Atmospheric Visibility Distance

A. Koschmieder's Law and Meteorological Visibility Distance

In the atmosphere, visible light is mainly attenuated by the scattering phenomenon characterized by an extinction coefficient k. The phenomenon is particularly strong in fog and causes a luminous veil which impairs visibility in daytime [14]. In 1924, Koschmieder [13] established a simple relationship between the apparent luminance L of an object at a distance d, and its intrinsic luminance L_0:

$$L = L_0 e^{-kd} + L_f(1 - e^{-kd}) \tag{1}$$

where L_f denotes the luminance of background sky. Based on these results, Duntley [13] derived a law for the atmospheric attenuation of contrasts:

$$C = \frac{|L - L_f|}{L_f} = C_0 e^{-kd} \tag{2}$$

where C designates the apparent contrast at distance d and C_0 the intrinsic contrast of the object against the sky. The CIE [1] adopted a contrast threshold of 5% to define V_{met}, the "meteorological" visibility distance, defined as the greatest distance at which a black object ($C_0 = 1$) of suitable dimensions can be recognized by day against the horizon sky:

$$V_{met} = -\frac{1}{k}\log(0.05) \simeq \frac{3}{k} \tag{3}$$

To our knowledge, Koschmieder's model is consistent with our application apart from the fog inhomogeneities which are not taken into account.

B. Mobilized and Mobilizable Visibility Distances

We now define V_{mob}, the "mobilized" visibility distance: the distance to the most distant visible object on the road surface, which is assumed to be black or at least dark. V_{mob} has to be compared with V_{max}, the "mobilizable" visibility distance: the maximum distance at which a potential object on the road surface would be visible. V_{max} can be expressed as a function

of V_{met} and the contrast threshold C_{BW} between a "white" object and a "black" object to be visible. Using (1) and (2), we show the following [5]:

$$V_{max} = -\frac{V_{met}}{3} \log \left[\frac{C_{BW}}{1 + C_{BW}} \right] \tag{4}$$

We obtain the value $\tilde{C}_{BW}$ so that $V_{max} = V_{met}$:

$$\tilde{C}_{BW} = \frac{1}{e^3 - 1} \approx 5\% \tag{5}$$

Thus, by using a 5% contrast threshold, V_{max} is very close to V_{met}. It follows that we have the following relationship between mobilized, mobilizable and meteorological visibility distances in daytime:

$$V_{mob} \leq V_{max} \approx V_{met} \tag{6}$$

Finally, (6) means that the maximum visibility distance of a white object located on a black road surface is the same one that a black object observed against its background sky.

III. In-vehicle Estimation of Atmospheric Visibility Distance

We developed two methods in order to estimate the atmospheric visibility distance through use of in-vehicle cameras.

A. Fog Detection and Estimation of Meteorological Visibility Distance

1) Theoretical Framework: By adopting the hypothesis of a flat road, which makes it possible to associate a distance d with each line v of a digital image, the distance d is expressed as follows:

$$d = \begin{cases} \frac{\lambda}{(v - v_h)} & \text{if } v > v_h \\ \infty & \text{if } v \leq v_h \end{cases} \tag{7}$$

where v_h is the vertical position of the horizon in the image plane and $\lambda = \frac{H\alpha}{\cos^2 \theta}$ depends on intrinsic and extrinsic parameters of the camera. H denotes the camera mounting height, θ the pitch angle and α the ratio between the focal length and the pixel size.

If a change of variable based on (7) is carried out, we can take twice the derivative of (1) with respect to v and obtain:

$$\frac{d^2 L}{dv^2} = k \frac{\lambda (L_0 - L_f)}{(v - v_h)^3} e^{-k \frac{\lambda}{v - v_h}} \left(\frac{k\lambda}{v - v_h} - 2 \right) \tag{8}$$

$\frac{d^2L}{dv^2}$ has two zeros, only one of which is useful: $k = \frac{2(v_i - v_h)}{\lambda}$, where v_i denotes the position of the inflection point. Hence, parameter k of Koschmieder's law is obtained once v_i is known. Finally, by virtue of (3), we are able to deduce V_{met}:

$$V_{met} = \frac{3\lambda}{2(v_i - v_h)} \tag{9}$$

2) Method Implementation: To implement this method, we measure the median intensity on each line of a vertical band in the image. As this band should only take into account a homogeneous area and the sky, we identify a region within the image which displays minimal line-to-line gradient variation when crossed from bottom to top using a region growing algorithm. A vertical band is then selected in the segmented area. Thus, we obtain the vertical variation of the intensity in the image, and deduce V_{met} using (8). An example of meteorological visibility distance computation is given on Fig. 1a. This method was patented in 2002 [12]. Details can be found in [6].

B. Estimation of Mobilized Visibility Distance

The previous method leads to good results in daytime foggy weather. In order to extend the range of covered meteorological situations, we developed a different approach, which consists in estimating V_{mob}. In this aim, three tasks must be achieved which are successively described.

1) Estimation of Local Contrasts above 5%: Based on a classical image segmentation method [9], we developed an original method which computes local contrasts above 5%. It consists in scanning the image using small windows, which are segmented by searching the border which maximizes Weber's contrast [2] between the two parts of the window. This method was compared with to the rare existing methods and proves to be precise as well while making less false detections [7].

2) Computation of a Precise Depth Map of the Road Surface using Stereovision: Stereovision allows depth information to be recovered by triangulation. However, a classical disparity map may contain numerous false matches, which prevents to use it as a depth map of the environment. The "v-disparity" transform, in which the detection of straight lines is equivalent to the detection of planes in the scene, allows to compute in two passes a high-quality depth/disparity map of the road surface [10]. We use it for estimating V_{mob}.

3) Fast Combination of both Information: This disparity map contains depth information of the road surface only. Consequently, if this is scanned from top to bottom, the objects encountered in the road surface are nearer and nearer the equipped vehicle. Estimating V_{mob} consists therefore in scanning the disparity map from top to bottom, starting at the horizon line and computing the contrast for each pixel of known disparity. Once the process finds a pixel with a contrast higher than 5%, computation ends. On the basis of the disparity of this pixel, it is possible to obtain V_{mob}. An example of V_{mob} computation is given in Fig. 1b. This method was patented in 2004 [4]. Details can be found in [5].

[Figure 1 about here.]

IV. Experimental Protocol based on a Dedicated Site

A. Setting up of a Dedicated Site

So far, our methods were only qualitatively evaluated, through a subjective analysis of the mean and standard deviation of measures in the cases of different rides assuming constant adverse visibility conditions. Quantitative assessment has not been endeavored yet, due to the lack of a reference visibility sensor. To fill this gap, we equipped our test track in Versailles (France) with five large specific targets, located between 65m and 200m from the cameras onboard the stationed vehicle (cf. Tab. I). An additional mobile target is used at a closer range when the fog is very dense. The idea is to take pictures of these targets in adverse weather conditions and to estimate the meteorological visibility distance based on the attenuation of their contrast. This static measurement, which uses reference targets, can then be compared on the same images to the results of our onboard dynamic techniques, which require no reference. The targets are designed for maximum intrinsic contrast as illustrated in Fig. 2b. A picture of the validation site in sunny weather conditions is given in Fig. 2a. Compared with [8], we see two advantages to our approach. First, the different targets have the same apparent size in the image, so as to take only the effects of the atmosphere into account. Second, the white and the black parts of each target have the same size, so as to have the same a priori confidence in the estimation of their intensities.

[Table 1 about here.]

[Figure 2 about here.]

B. Using the targets

We consider the black part of two black targets located at distances d_1 and d_2 from the camera. We assume that they have a null intrinsic luminance ($L_B(0) = 0$). In daytime fog, according to Koschmieder's law (1), their apparent luminances are:

$$\begin{cases} L_B(d_1) &= (1 - e^{-kd_1})L_f \\ L_B(d_2) &= (1 - e^{-kd_2})L_f \end{cases} \tag{10}$$

Taking the ratio $r = \frac{L_B(d_1)}{L_B(d_2)}$ of these values allows us to deduce the value of the extinction coefficient k in different ways:

$$k = \begin{cases} -\frac{1}{d_1}\log\left[r-1\right] & \text{if } d_2 = 2d_1 \\ -\frac{1}{d_1}\log\left[\frac{\sqrt{4r-3}-1}{2}\right] & \text{if } d_2 = 3d_1 \\ -\frac{1}{d_1}\log\left[\frac{\left(r-1\right)\left(\sqrt{r+3}-\sqrt{r-1}\right)^2}{4}\right] & \text{if } d_2 = \frac{3}{2}d_1 \end{cases} \tag{11}$$

An alternative technique consists in using the white and the black parts of the targets, whose apparent luminances $L_W(d)$ and $L_B(d)$ are given by Koschmieder's Law (1):

$$\begin{cases} L_W(d_1) - L_B(d_1) &= e^{-kd_1}L_{W_0} \\ L_W(d_2) - L_B(d_2) &= e^{-kd_2}L_{W_0} \end{cases} \tag{12}$$

Again taking the ratio of these values, we deduce the value of extinction coefficient k:

$$k = -\frac{1}{d_2 - d_1}\log\left[\frac{L_W(d_2) - L_B(d_2)}{L_W(d_1) - L_B(d_1)}\right] \tag{13}$$

An estimation $\mathcal{V}(k)$ of the variance of k is associated with each formula (11) or (13) and is expressed by:

$$\mathcal{V}(k) \approx \mathcal{V}_I \sum \left[\frac{\partial k}{\partial L_{B,W}(d_{1,2})}\right]^2 \tag{14}$$

where $\mathcal{V}_I$ is the variance on the pixel value due to the digitalization of the pictures, assuming a gaussian centered distribution with a standard deviation of $\frac{1}{2}$. From (3), we deduce the variance of V_{met}:

$$\mathcal{V}(V_{met}) \approx \left[\frac{V_{met}}{k}\right]^2 \mathcal{V}(k) \tag{15}$$

Thus, from previous equations, we have different estimates of the meteorological visibility distance and we have an evaluation of the variance of these estimates. Assuming that the measurements are not correlated, these estimates are optimally averaged using the variances:

$$\hat{V}_{met} = \frac{\sum_i \frac{V_{met_i}}{\mathcal{V}(V_{met_i})}}{\sum_i \frac{1}{\mathcal{V}(V_{met_i})}} \tag{16}$$

The variance of this estimator is: $\left(\sum_i \frac{1}{\mathcal{V}(V_{met_i})}\right)^{-1}$.

[Figure 3 about here.]

C. Protocol Validation on Photometric Simulations

To check the validation process, we first ensure that the site suits our objectives and that the equations which were presented in the previous section are relevant for estimating the meteorological visibility distance. In this aim, using a photometric model of fog effects on vision based on Koschmieder's Law and detailed in [3], we simulated pictures of a virtual make-up of our validation site in daytime fog, for different values of V_{met}: 33m, 66m, 100m, 133m, 166m and 200m (cf. Fig. 3).

[Table 2 about here.]

Tab. IIA gives the values of $\widehat{V}_{met}$ obtained thanks to averages of estimates (11). Tab. IIB gives the values of $\widehat{V}_{met}$ obtained thanks to averages of (13). Firstly, some results at the bottom of the tables are bad. The reason for that is the round-off caused by the digital nature of the simulated images. Thereafter, the logarithmic formula is more sensitive to the weak differences in intensity of the targets far away, than with the great differences in intensity of the closer targets. The estimated visibility distance is thus necessarily worst using the most distant targets. All these considerations are confirmed by the standard deviation values, which are given between brackets in Tab. II. Secondly, the standard deviations in Tab. IIA are smaller than in Tab. IIB. Unfortunately, the method seems to be skewed, because the estimated visibility distance is biased and always smaller than the ground truth. This may be due to the fact that the targets are not really black, as is assumed for establishing (11). In our simulations, we implemented a reflectance factor of 1% in order to stick to reality. Consequently, in the following tests, we will only rely on average of (13) to compute the reference measurement $\hat{V}_{met}$.

V. Experimental validation

A. Construction of a Reference Data Set

[Figure 4 about here.]

Some images of the validation site have been grabbed under various weather conditions: sun, light rain, haze, snow fall, fog, etc. $\widehat{V}_{met}$ is estimated from each image. However, Indeed, in our camera configuration (B&W PAL camera, H=1.4m, α=1000, θ=8.5°), the size of a pixel located beyond 250m on a flat road is greater than 50m, which already represents a quite important uncertainty. We thus compare the methods presented in section III, only if $\hat{V}_{met} < 250\text{m}$. Consequently, we only focus on foggy conditions. We have approximately 60 pictures of our validation site under foggy conditions. On some pictures, a car (light on/off) and a pedestrian are set on the road at various distances of the equipped vehicle in order to test the robustness of the methods. Some samples of the processed images are given in Fig. 4. We have computed $\hat{V}_{met}$ and its variance for each image. The visible targets are selected interactively. In Fig. 5, $\hat{V}_{met}$ is plotted for each image (marked with a +) as well as the interval $[\hat{V}_{met} - \sigma, \hat{V}_{met} + \sigma]$ (vertical segment). Unfortunately, due to the instability of the fog phenomenon, it is difficult to assume that time consecutive images represent the same visibility conditions, which could have been used to reduce the variance.

[Figure 5 about here.]

B. Results and Discussion

[Figure 6 about here.]

To evaluate the accuracy of our methods, we estimated for each image the reference visibility distance $\hat{V}_{met}$ obtained from the targets with the method described in section IV-B and the meteorological visibility distance V_{met} obtained with the method described in section III-A and the mobilized visibility distance V_{mob} obtained with the method described in section III-B.

In Fig. 6, we plot V_{met} versus $\hat{V}_{met}$ as well as the least-squares line, whose equation is on the graph. The linear correlation coefficient between both measurements is good (about 97%). By neglecting the offset of the least-squares line, the method seems to slightly underestimate the visibility distance. This can be due to the fact that the road is actually not plane and that

the calibration of the horizon line is inaccurate. In Fig. 7, we plot V_{mob} versus $\hat{V}_{met}$, as well as the least-squares line. The linear correlation coefficient between both measurements is as good as for Fig. 6 (about 97%). The second method also slightly underestimates the visibility distance. But, in this case, this is quite normal. Indeed, according to (6), V_{mob} should be always inferior or equal to V_{met} and consequently to $\hat{V}_{met}$. Moreover, both methods seem to be robust to the presence of obstacles in the field of view of the camera. Finally, different error estimations between reference and in-vehicle measurements are given in Tab. III. The accuracy of in-vehicle methods is approximately 10%.

[Figure 7 about here.]

Even if some hypotheses must still be quantitatively validated, the results are satisfactory, taking into account the fact that experimental validation of such methods is very difficult. Indeed, grabbing pictures under natural foggy conditions is a tough task, because we do not control the weather conditions and the fog homogeneity. Moreover, our validation site is a prototype. Consequently, it has some minor imperfections: the road is not plane and is not "black", contrary to our assumptions. We also had to make a compromise between the size of the targets and their wind resistance. Using bigger targets would have led to a better estimation of $\hat{V}_{met}$, however it was not physically possible. Nevertheless, a camera with a better resolution could improve the reference estimates. Indeed, if the camera resolution is improved by a factor n, the number of pixels belonging to a target is increased by a factor n^2 since all the targets have the same size in the image. By assuming that the pixels are independent from each other and keep a constant sensitivity, the uncertainty on $\hat{V}_{met}$ is reduced by a factor $\frac{1}{\sqrt{n^2}} = \frac{1}{n}$. Finally, a radiometric calibration of the camera would also slightly improve the correlation of the data. In the future, it would be interesting to test the methods with a better camera and to have a transmissometer, so as to be able to evaluate the meteorological visibility distance with a sensor dedicated to the measurement of the extinction coefficient of the atmosphere. The dynamic validation of the methods remains a challenging task.

[Table 3 about here.]

VI. Conclusion

In this article, we presented a measurement framework for different atmospheric visibility distances which are defined. A link between the different distances is built. Two onboard techniques to measure them are briefly presented. Then, the problem of the validation of such techniques is discussed. We proposed a solution based on a static calibration using a dedicated site with reference targets. The graphic design retained for the targets and the geometry of the site is presented. Then, the validation process is presented and applied on photometrically simulated pictures of the site. Then, we compare the results of the onboard techniques and the static one on actual pictures of the site. The first results are satisfactory and are in agreement with the theory. The validation site which is presented is quite well adapted to estimate the meteorological visibility distance. Finally, ideas for improving the results are indicated.

References

[1] *International Lighting Vocabulary*. Commission Internationale de l'Éclairage, 1987, no. 17.4.

[2] T. Cornsweet, *Visual perception*. Academic Press, 1970.

[3] E. Dumont and V. Cavallo, "Extended Photometric Model of Fog Effects on Road Vision," *Transportation Research Records*, no. 1862, pp. 77–81, 2004.

[4] N. Hautière, R. Labayrade, and D. Aubert, "Dispositif de mesure de distance de visibilité," French patent 0411061, LCPC/INRETS, oct 2004.

[5] ——, "Real-time disparity contrast combination for onboard estimation of the visibility distance," *IEEE Transactions on Intelligent Transportation Systems*, vol. 7, no. 2, pp. 201–212, June 2006.

[6] N. Hautière, J.-P. Tarel, J. Lavenant, and D. Aubert, "Automatic fog detection and estimation of visibility distance through use of an onboard camera," *Machine Vision and Applications Journal*, vol. 17, no. 1, pp. 8–20, April 2006.

[7] N. Hautière, D. Aubert, and M. Jourlin, "Measurement of local contrast in images, application to the measurement of visibility distance through use of an onboard camera," *Traitement du Signal*, vol. 23, no. 2, pp. 145–158, 2006.

[8] T. M. Kwon, "Atmospheric Visibility Measurements using Video Cameras: Relative Visibility," University of Minnesota Duluth, Tech. Rep., July 2004.

[9] R. Köhler, "A segmentation system based on thresholding," *Graphical Models and Image Processing*, vol. 15, pp. 319–338, 1981.

[10] R. Labayrade and D. Aubert, "In-vehicle obstacles detection and characterization by stereovision," in *1st Int. Workshop on In-Vehicle Cognitive Computer Vision Systems, Graz, Austria*, November 2003.

[11] R. Labayrade, D. Aubert, and J.-P. Tarel, "Real Time Obstacle Detection in Stereovision on non Flat Road Geometry through v-disparity Representation," in *IEEE Intelligent Vehicle Symposium, Versailles, France*, 2002.

[12] J. Lavenant, J.-P. Tarel, and D. Aubert, "Procédé de détermination de la distance de visibilité et procédé de détermination de la présence d'un brouillard," French patent 0201822, LCPC / INRETS, Feb 2002.

[13] W. Middleton, *Vision through the atmosphere*. University of Toronto Press, 1952.

[14] G. Paulmier, “Luminance Evaluation in Daytime Fog,” *Transportation Research Records*, no. 1862, pp. 82–88, 2004.

[15] PREDIT, “ARCOS: Research Action for Secure Driving,” http://www.arcos2004.com.

LIST OF FIGURES

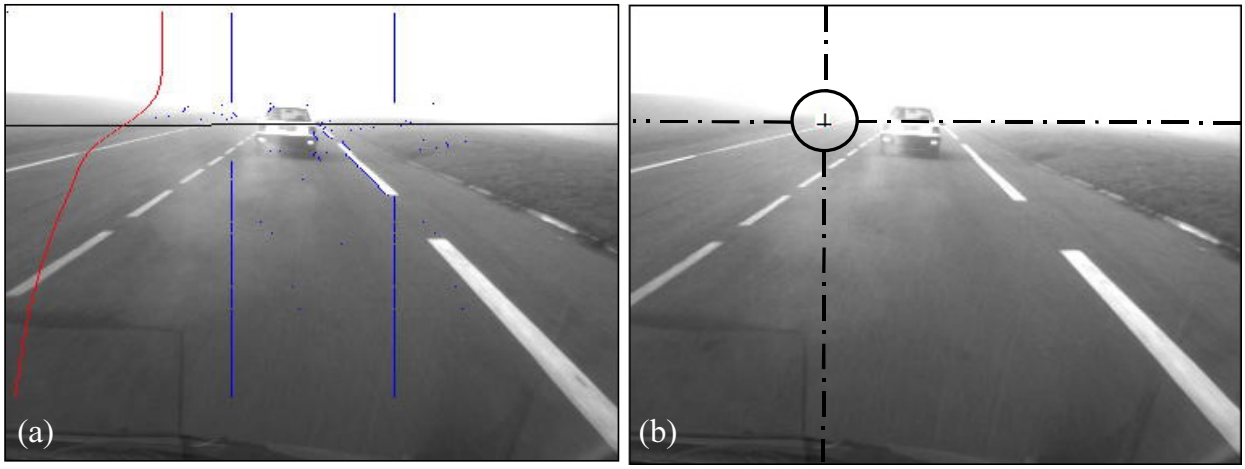

Fig. 1. (a) Estimation of the meteorological visibility distance using the technique based on inflection point detection. The curve on the left depicts the median intensity measured on the vertical band. The visibility distance is represented through use of a horizontal black straight line. (b) Estimation of the mobilized visibility distance. The most distant window having a contrast above 5%, on which a disparity point is known, is painted white. The point is represented with a black cross on the white window.

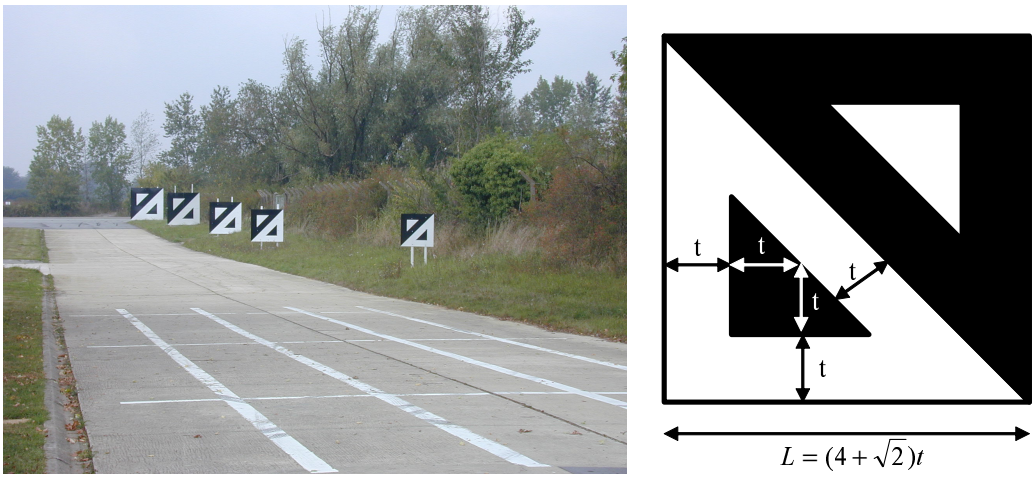

(a) (b)

Fig. 2. (a) Actual picture of the validation site dedicated to visibility measurement, taken in sunny weather conditions. (b) Graphic design of the reference targets.

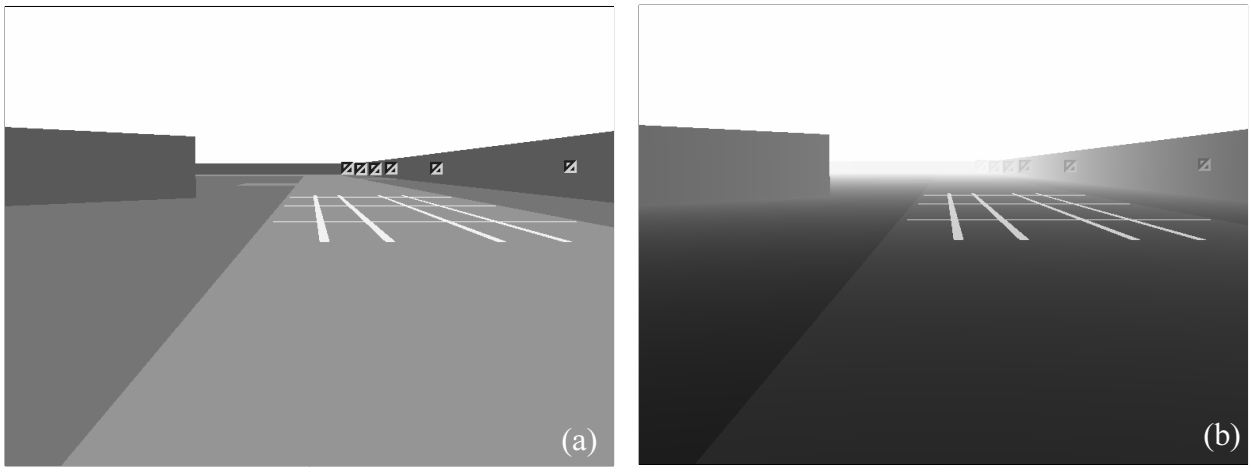

Fig. 3. Photometrically simulated pictures of the validation site: (a) without fog, (b) with fog: $V_{met} = 200m$.

Fig. 4. Images grabbed on the validation site under various weather conditions and with occlusions of the road: (a) sunny weather $\hat{V}_{met} \approx 5000$m; (b) haze $\hat{V}_{met} \approx 2000$m; (c) snow fall $\hat{V}_{met} \approx 1000$m; (d) light fog $\hat{V}_{met} \approx 255$m (five visible targets); (e)(f) dense fog + obstacles $\hat{V}_{met} \approx 120$m (two or three visible targets).

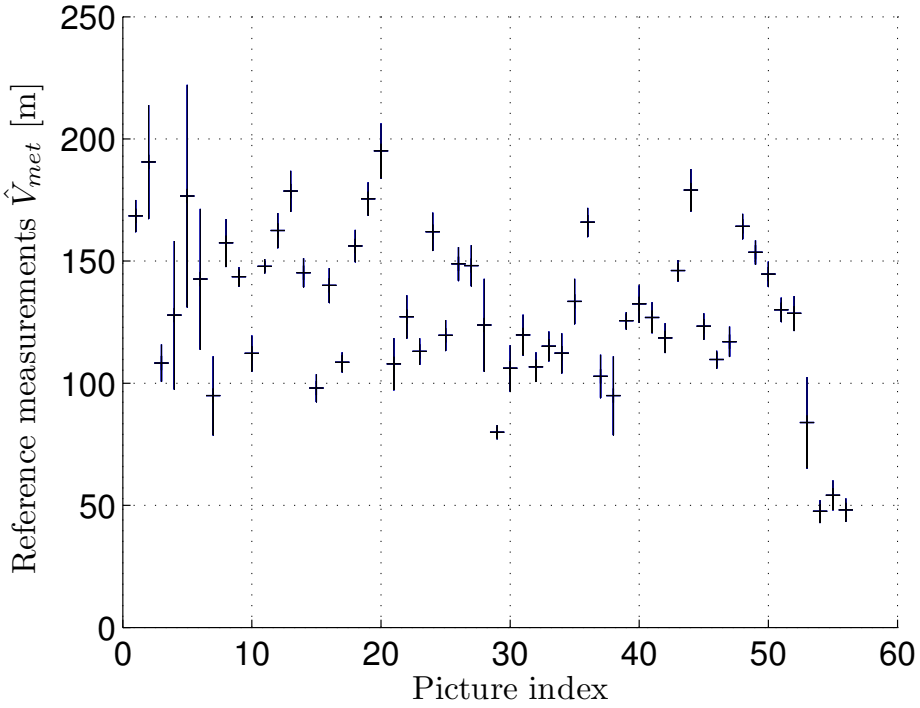

Fig. 5. Estimation of $\hat{V}_{met}$ marked with a + for each image of the data set and interval $[\hat{V}_{met}-\sigma, \hat{V}_{met}+\sigma]$ (vertical segment).

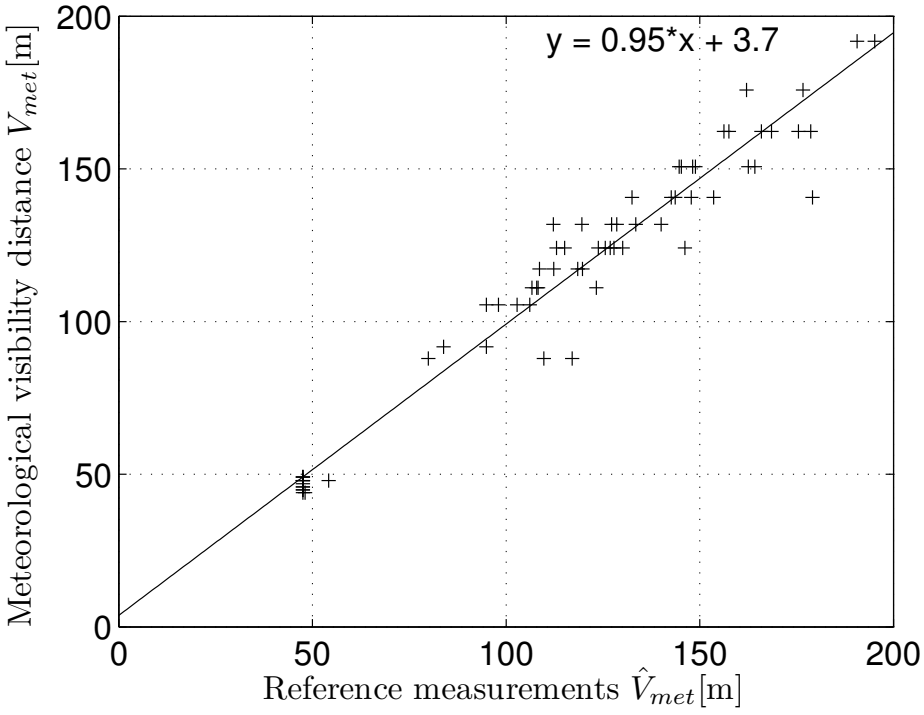

Fig. 6. Points: estimation of the meteorological visibility distance V_{met} versus the reference visibility distance $\hat{V}_{met}$ obtained thanks to the reference targets. Line: correlation line of the points, whose equation is shown in the graph. The linear correlation coefficient is about 97%.

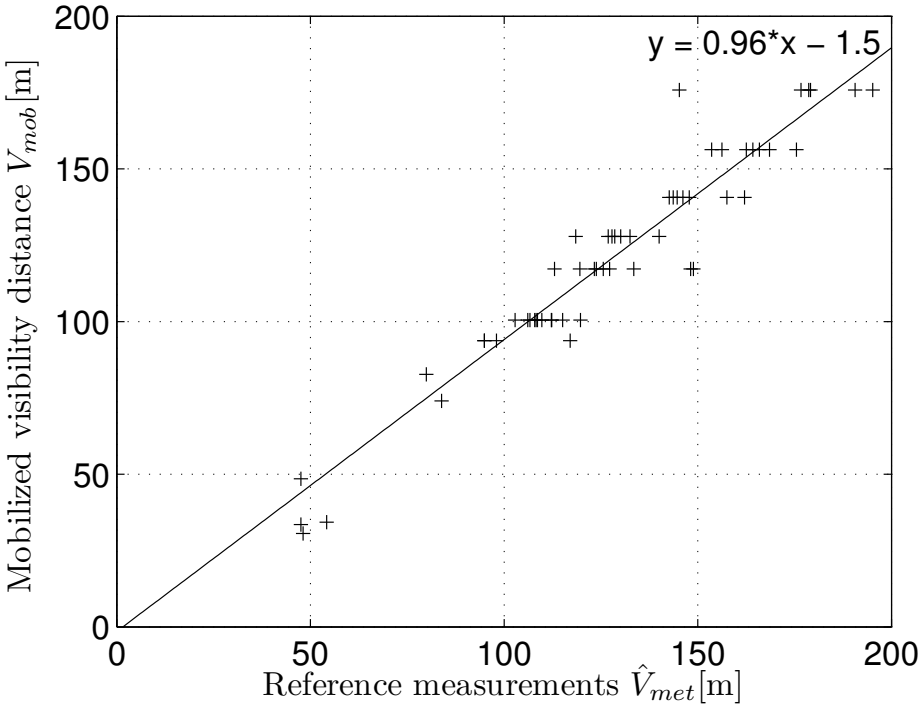

Fig. 7. Points: estimation of the mobilized visibility distance V_{mob} versus the reference visibility distance $\hat{V}_{met}$ obtained thanks to the reference targets. Line: least-squares line of the points, whose equation is shown in the graph. The linear correlation coefficient is also about 97%.

LIST OF TABLES

Target index	1	2	3	4	5	6
Distance [m]	0-35	65.2	97.6	130.7	162.4	195
L [m]	0.5	1	1.5	2	2.5	3
t [m]	0.1	0.19	0.28	0.37	0.47	0.56

TABLE I

DISTANCE AND DIMENSIONS L, t (SEE FIG. 2B) OF THE DIFFERENT REFERENCE TARGETS ON THE VALIDATION SITE.

(A)

$\widehat{V}_{met}(\sigma)$ **[m]**		V_{met} **[m]**				
		200	**166**	**133**	**100**	**66**
couple of targets	$1 \rightarrow 2$	172 (5)	144 (3)	119 (2)	92 (2)	61 (1)
	$1 \rightarrow 3$	183 (3)	151 (2)	124 (2)	95 (1)	-
	$2 \rightarrow 3$	199 (5)	161 (4)	132 (3)	100 (2)	-
	$2 \rightarrow 4$	197 (3)	162 (2)	132 (2)	-	-
	$2 \rightarrow 6$	198 (2)	-	-	-	-
	$3 \rightarrow 6$	197 (3)	-	-	-	-
	$4 \rightarrow 6$	199 (4)	-	-	-	-
	$\widehat{V}_{met}$	194 (1)	155 (1)	126 (1)	95 (1)	61 (1)

(B)

$\widehat{V}_{met}$ (σ) **[m]**		V_{met} **[m]**				
		200	**166**	**133**	**100**	**66**
couple of targets	$1 \rightarrow 2$	203 (14)	170 (12)	138 (10)	103 (9)	74 (1)
	$1 \rightarrow 3$	198 (10)	173 (10)	135 (10)	103 (11)	-
	$1 \rightarrow 4$	201 (11)	162 (11)	138 (13)	-	-
	$1 \rightarrow 5$	189 (13)	172 (15)	-	-	-
	$1 \rightarrow 6$	203 (17)	-	-	-	-
	$2 \rightarrow 3$	194 (21)	176 (23)	133 (20)	103 (23)	-
	$2 \rightarrow 4$	200 (16)	158 (16)	138 (20)	-	-
	$2 \rightarrow 5$	184 (17)	172 (20)	-	-	-
	$2 \rightarrow 6$	203 (21)	-	-	-	-
	$3 \rightarrow 4$	206 (39)	143 (29)	142 (46)	-	-
	$3 \rightarrow 5$	180 (25)	170 (31)	-	-	-
	$3 \rightarrow 6$	207 (30)	-	-	-	-
	$4 \rightarrow 5$	160(42)	210 (105)	-	-	-
	$4 \rightarrow 6$	207(46)	-	-	-	-
	$5 \rightarrow 6$	294 (214)	-	-	-	-
	$\widehat{V}_{met}$	197 (4)	168 (5)	137 (6)	103 (7)	74 (11)

TABLE II

ESTIMATED VISIBILITY AND VARIANCE (BETWEEN BRACKETS) ON SIMULATED PICTURES USING THE REFERENCE TARGETS AND (A) AVERAGE ESTIMATES (11) OR (B) AVERAGE ESTIMATES (13).

		V_{met}	V_{mob}
Average error [m]	$\frac{1}{n}\sum_{i=1}^{n}\lvert\hat{V}_i - V_i\rvert$	6.3	8.7
Absolute global error [m]	$\sqrt{\frac{1}{n}\sum_{i=1}^{n}(\hat{V}_i - V_i)^2}$	9.3	11.7
Relative global error [%]	$\sqrt{\frac{\sum_{i=1}^{n}(\hat{V}_i - V_i)^2}{\sum_{i=1}^{n}\hat{V}_i^2}}$	8	9.3

TABLE III

AVERAGE, ABSOLUTE GLOBAL AND RELATIVE ERRORS BETWEEN REFERENCE AND IN-VEHICLE MEASUREMENTS.